Global Change Biology

Global Change Biology (2017) **23**, 2499–2508, doi: 10.1111/gcb.13532

Will phenotypic plasticity affecting flowering phenology keep pace with climate change?

BRYCE A. RICHARDSON[1], LINDSAY CHANEY[2]*, NANCY L. SHAW[3] and SHANNON M. STILL[4]

[1]*USDA Forest Service, Rocky Mountain Research Station, Provo, UT 84606, USA,* [2]*Plant and Wildlife Sciences, Brigham Young University, Provo, UT 84602, USA,* [3]*USDA Forest Service, Rocky Mountain Research Station, Boise, ID 83702, USA,* [4]*UC Davis Arboretum, University of California, Davis, 1 Shields Ave., Davis, CA 95616, USA*

Abstract

Rising temperatures have begun to shift flowering time, but it is unclear whether phenotypic plasticity can accommodate projected temperature change for this century. Evaluating clines in phenological traits and the extent and variation in plasticity can provide key information on assessing risk of maladaptation and developing strategies to mitigate climate change. In this study, flower phenology was examined in 52 populations of big sagebrush (*Artemisia tridentata*) growing in three common gardens. Flowering date (anthesis) varied 91 days from late July to late November among gardens. Mixed-effects modeling explained 79% of variation in flowering date, of which 46% could be assigned to plasticity and genetic variation in plasticity and 33% to genetics (conditional $R^2 = 0.79$, marginal $R^2 = 0.33$). Two environmental variables that explained the genetic variation were photoperiod and the onset of spring, the Julian date of accumulating degree-days >5 °C reaching 100. The genetic variation was mapped for contemporary and future climates (decades 2060 and 2090), showing flower date change varies considerably across the landscape. Plasticity was estimated to accommodate, on average, a ±13-day change in flowering date. However, the examination of genetic variation in plasticity suggests that the magnitude of plasticity could be affected by variation in the sensitivity to photoperiod and temperature. In a warmer common garden, lower-latitude populations have greater plasticity (+16 days) compared to higher-latitude populations (+10 days). Mapped climatypes of flowering date for contemporary and future climates illustrate the wide breadth of plasticity and large geographic overlap. Our research highlights the importance of integrating information on genetic variation, phenotypic plasticity and climatic niche modeling to evaluate plant responses and elucidate vulnerabilities to climate change.

Keywords: *Artemisia tridentata*, common garden, genotype–environment interaction, mixed-effects model, photoperiod, range shifts

Received 3 June 2016; revised version received 28 September 2016 and accepted 1 October 2016

Introduction

A well-established relationship exists between temperature and plant phenological responses. Studies have shown that climate warming is concomitant with phenological change (Parmesan & Yohe, 2003; Menzel *et al.*, 2006; Gordo & Sanz, 2010). However, it is also known that the magnitude of phenological trait responses can vary among species (Körner & Basler, 2010; Laube *et al.*, 2014) and among populations within species (Viveros-Viveros *et al.*, 2009; Wilczek *et al.*, 2009; Haggerty & Galloway, 2010; Vitasse *et al.*, 2013; Anderson & Gezon, 2014). Trait variation can be attributed to genes, the environment (i.e., phenotypic plasticity) and genetic variation in plasticity (i.e., genotype–environment interaction, G × E). Therefore, understanding the role genetic factors, phenotypic plasticity, and G × E is a key to evaluate fitness, adaptation and vulnerabilities to environmental change. Information that is critical to guide seed transfer and assisted migration.

The degree of phenotypic plasticity expressed by a trait can have an important bearing on plant fitness under a changing climate (Shaw & Etterson, 2012; Franks *et al.*, 2013). Common garden and reciprocal transplant studies are an effective approach to untangle adaptive genetic responses and phenotypic plasticity (Langlet, 1971; Morgenstern, 1996). A common garden controls for environmental effects on a phenotype, allowing for a more accurate observation of the genetic effects. The use of multiple common gardens allows comparisons of phenotypes across environments, providing an evaluation of phenotypic plasticity and G × E (Pigliucci, 2005). Moreover, mixed-effects models have been shown to be an effective analytical tool for common garden studies (e.g., Joyce & Rehfeldt,

Correspondence: Bryce A. Richardson, tel. +1 801 356 5112, fax +1 801 375 6968, e-mail: brichardson02@fs.fed.us

* Present address: Department of Biology, Snow College, Ephraim, UT 84627, USA

Published 2016.

2013; Rehfeldt *et al.*, 2014b), equipped to parse fixed and random effects and handle unbalanced study designs and nonnormal data (Bolker *et al.*, 2009; Schielzeth & Nakagawa, 2012).

Flower phenology can affect gene flow, biotic and abiotic interactions and other life history traits, potentially affecting fitness (Elzinga *et al.*, 2007; Galloway & Burgess, 2012; Franks, 2015). Temperature and photoperiod cues typically initiate flowering, and the genetic processes and pathways are well understood in model plant species (Amasino, 2010; Blackman *et al.*, 2011; Song *et al.*, 2015). However, limited information exists on how genetic, phenotypic plasticity and G × E flowering components will respond to climate change (but see Franks *et al.*, 2007; Wilczek *et al.*, 2010; Anderson *et al.*, 2012). Here, we examine flower phenology variation for 1018 individuals among 52 populations and three subspecies of big sagebrush (*Artemisia tridentata*, Asteraceae) when grown in three common gardens of widely varying environments. This species is an autumn-flowering, wind-pollinated, xerophytic shrub, widely distributed in the cold deserts of western North America, spanning approximately 16^{o} latitude and an elevation range of 3000 m. In this study, we develop a model that explains the variation in flower phenology and partition genetic, phenotypic plasticity and G × E. The genetic contribution of flowering date is mapped for three time periods: contemporary, mid-century and end-century. These time periods serve to estimate the flowering date change to evaluate the magnitude and variation in plasticity. Using these data, we address the following questions: (i) How much trait variation is explained by genetics, phenotypic plasticity and G × E, (ii) how much change in flowering date can be expected based on mid- and end-century climate change projections and (iii) can phenotypic plasticity, accounting for G × E, keep pace with climatic change?

Materials and methods

Sample collection and garden establishment

Big sagebrush seed was collected from 52 populations in the autumn of 2009. Seed collected from the same maternal plant was considered half-sibs and hereafter referred to as a family. Seed was cleaned using previously published methods (Richardson *et al.*, 2015) and placed into a −20 °C freezer until sowing into six-inch cone-tainers. Seedlings were kept in a greenhouse for approximately 3 months, hardened outdoors for 1 week and planted into common gardens in the spring of 2010. Common garden locations were chosen to be representative of the varied climates occupied by different subspecies. These gardens included the following: Orchard, Idaho, a warm–dry basin site occupied by *A.t. wyomingensis* and *tridentata*; Ephraim, Utah, a cold–dry basin site with deep soils occupied by *A.t. tridentata*; and Majors Flat, Utah, a cold–wet mountain site occupied by *A.t. vaseyana*. Ephraim and Majors Flat are 8 km apart, but Majors Flat is 420 m higher in elevation. Due to differences in climate, the Orchard and Ephraim gardens were planted in late April, and Majors Flat was planted in early June of 2010. Therefore, the seedling rearing procedure was delayed for Majors Flat to ensure seedlings were approximately the same age when planted. Assignment of subspecies (*tridentata*, *vaseyana*, *wyomingensis*) was completed based on morphology (height and stature), cytotype (ploidy), UV fluorescence (Stevens & McArthur, 1974), molecular genetic analyses (Richardson *et al.*, 2012) and volatile organic compounds (Jaeger *et al.*, 2016). Flow cytometry was conducted on at least one member of each family using previously published methods (Richardson *et al.*, 2012) to determine cytotype. Geographic coordinates, sample size and subspecies information for each population are summarized in Table S1.

Prior to planting, the gardens were lightly tilled and a perimeter fence was constructed to exclude herbivory from ungulates. Fencing also extended 0.7 m below ground to discourage rodent herbivory. Fencing was placed at least 4.5 m away from the border rows to minimize effects from drifting snow. A completely randomized design was used for each garden. Additional nonexperimental plants were used in a border row along the perimeter to eliminate edge effects. Plant spacing was 1.5 m between rows and 1 m within rows. To ensure establishment, plants were watered periodically during the first growing season (May to August, 2010).

Data collection

Flower phenology was estimated at all three gardens in 2012, 2 years after planting. Because anthesis occurs over several days in *A. tridentata*, we estimated the Julian date (i.e., day of year) in which anthesis reached 50% for each plant based on visual inspection. Flowering dates were scored from late July to late November in intervals of 7–10 days. If 50% anthesis took place between weekly observations, the average daily rate of flower opening was calculated by subtracting the difference in the previous and current observations and then divided by the days passed between observations. This daily value was added to the previous weeks estimate until 50% anthesis for each individual plant was reached.

Population–climate estimates

Population source–climate variables estimated from thin-plate spline smoothing procedures (ANUSPLINE v4.3; Hutchinson, 2004) were obtained using the latitude, longitude and elevation of each population (Crookston & Rehfeldt, 2008). Climate estimates were projected on a 0.0083^{o} resolution gridded surface (~1 km^2) based on weather station data from 1961 to 1990 (Rehfeldt, 2006). A total of 41 predictor variables were used. This included 20 variables describing annual and seasonal temperature and precipitation estimates, 20 interactions of temperature and precipitation (Crookston & Rehfeldt, 2008) and the addition of latitude as a surrogate for photoperiod.

The data table used in the analysis and the R code can be found at https://github.com/brichardsonfs/flower.

Model selection and statistical analysis

To describe the variation in flowering time of a population, a linear mixed-effects model (LMM) was fitted using the lmer function from the LME4 package (Bates *et al.*, 2014) within the R statistical framework v 3.2.0 (R Core Team, 2015). A LMM was chosen over ANOVA because of its ability to quantify random effect groups and handle some sample unbalance among gardens due to mortality. A hierarchy, based on the experimental design, was used for random effects in the following descending order: garden, subspecies and population. Both population and subspecies were a full-factorial design among gardens. Garden effects were considered to be caused by environment, whereas interactions with species and population were considered to be caused by G × E. Family was not replicated within each garden and therefore was omitted as a random effect. Population source–environmental variables (climate and latitude) were specified as fixed effects and tested for clinal variation in flowering date. Prior to fitting a LMM, climate variables were culled based on two criteria: low correlation with the population mean flowering date and collinearity among the predictors. A minimum Pearson correlation coefficient with flowering date was set at $|r| > 0.5$. This process eliminated 27 of the 41 climate variables. A model including the remaining 14 climate variables and the garden effects were fitted into backward stepwise regression model using the step function in LMERTEST package (Kuznetsova *et al.*, 2016). Significance for random effects was calculated based on likelihood ratio chi-squared test, and significance for fixed effects was calculated using Satterthwaite's approximation for degrees of freedom. Fixed and random effects were eliminated from the model if $P > 0.05$. Finally, three models containing two and three fixed effect variables were compared with the ANOVA function (LMERTEST). We chose the most parsimonious, two-variable model with the lowest Bayesian information criteria. These variables included latitude, a surrogate for photoperiod and D100, the Julian date of degree-days >5 °C accumulating to 100. Conditional and marginal R^2 (Johnson, 2014) values were calculated with the r.squaredGLMM function in the MUMIN package (Bartoń, 2015). A conditional R^2 described the variation explained by both fixed and random effects, and a marginal R^2 described fixed effects alone.

Evaluating phenotypic plasticity

We calculate climatypes using an approach similar to Rehfeldt *et al.* (2014a,b) where a significance level of 0.2 is an appropriate estimate of determining genetic differences among populations with traits exhibiting clinal variation. Confidence intervals at 20% and 80% were estimated around the mean flowering date of each population using the CONFINT function in LME4 with 1000 parametric bootstraps. The upper and lower confidence intervals for the slopes (latitude and D100) and intercept were used to calculate the confidence intervals for each population (Table S2). Population–garden interaction, G × E, was extracted from the LMM using the RANEF function in LME4 package. These values were then plotted with latitude of the source populations at each garden using Pearson's correlation to infer interactions between temperature and photoperiod. The linear relationship between G × E and latitude at the Orchard garden, the warmest garden, was used as a guide to infer how warming temperatures (i.e., climate change) could affect the magnitude of plasticity for each population.

Mapping

To map predicted flowering date, the grid cell values of latitude and D100, which explain the genetic contribution, were run through linear regression function for the contemporary climate. The same process was followed for the mid- and end-century prediction, but D100 was updated based on the downscaled general circulation model (GCM) of decade 2060 (2056–2065) and 2090 (2086–2095) (Crookston & Rehfeldt, 2008). The GCMs used the Representative Concentration Pathway (RCP) 6.0 from the fifth assessment (AR5) of the IPCC/CMIP5 (http://cmip-pcmdi.llnl.gov/cmip5/). The RCP 6.0 represents a medium–high emissions scenario (van Vuuren *et al.*, 2011). This process was conducted using the YAIMPUTE package in R (Crookston & Finley, 2008) and mapped within a geographic window between 33^o and 55^o north and 100^o and 130^o west. Predicted flowering date was mapped within the bioclimatic niche model of Wyoming big sagebrush (*A.t. wyomingensis*) described in Still & Richardson (2015) with the niche model updated with the RCP 6.0, as discussed above. Because of the largely sympatric distribution of *A.t. wyomingensis* and *A.t. tridentata* at this spatial scale (McArthur & Sanderson, 1999), the bioclimatic niche model also incorporates the majority of *A.t. tridentata* niche. Because the subspecies variable was not significant and eliminated as a random effect in the LMM ($P = 0.4$), data from all three subspecies were used in mapping Julian date within the climatic niche of *A.t. wyomingensis*. Flowering date from the contemporary gridded surface was subtracted from the 2060 and 2090 surfaces using the raster calculator in ARCMAP v10.2 (ESRI, Redlands, CA, USA) to assess the predicted change in flowering date. Populations of *A.t. wyomingensis* collected from northern (Montana, MTW1) and southern (Utah, UTV2) regions of the species range served as reference points for developing climatypes. Intervals using the average phenotypic plasticity (13 days) and the G × E from the Orchard garden were created around the predicted population mean flowering date (Fig. S2). Climatypes were mapped using the methods discussed above.

Results

Artemisia tridentata population mean flowering date, Julian days elapsed before 50% anthesis, spanned 91 days among the three common gardens, occurring from late August (Julian date = 243) to late November (Julian date = 334). Flowering was on average 15 days later at the warmer, higher-latitude garden, Orchard, than at the colder, lower-latitude gardens, Majors Flat and Ephraim (Table 1, Fig. S1). On average, flowering spanned 45 days; however, considerable variability was observed within gardens. Flowering was most protracted at Orchard, occurring over 73 days compared to 25 days at Ephraim and 37 days at Majors Flat.

These flower phenology observations are supported by LMM results. Phenotypic plasticity (garden) and G × E (population × garden) accounted for the majority of random effect variances compared to the residual. Plasticity and G × E were highly significant (Table 2). Among fixed effects, the variable elimination procedure and model selection via Bayesian information criteria resulted in a model with two variables: latitude and D100, which measures photoperiod and the onset of spring, respectively. Latitude and D100 were highly significant in explaining genetic effects (Table 2). Both predictor variables were negatively associated with flowering date (Fig. 1). For example, plants originating 1° higher in latitude flowered 1.9 days earlier, and plants originating from locations with a one-day later spring (D100) flowered 0.35 days earlier.

The LMM explained 79% (conditional $R^2 = 0.79$) of the variation in flowering date. This variation can be further subdivided into genetic variation (fixed effects) and phenotypic plasticity and G × E (random effects), accounting for 33% (marginal $R^2 = 0.33$) and 46% of the variation, respectively. The phenotypic plasticity was assessed by estimating confidence intervals around the fixed effects parameters. Confidence intervals were ±13 days (SD = 1.7) when averaged among populations (Table S2). However, the effect of G × E (i.e., the variation in plasticity) depended on the latitude of the seed source and the environment (i.e., garden). At the warmer Orchard garden (Table 1), flowering date was more likely to be delayed among lower-latitude populations and early among higher-latitude populations, resulting in a negative association between G × E and latitude ($r = -0.49$, $P = 0.0005$). However, at the cold gardens these patterns were reversed (Fig. 2), resulting in a positive association between G × E and latitude at Majors Flat ($r = 0.52$, $P = 0.0002$) and Ephraim ($r = 0.28$, $P = 0.07$). To infer the effects of climate warming on plasticity, the average plasticity among populations (±13 days) was adjusted based on the linear model at the Orchard garden (Fig. 2). This resulted in larger G × E at lower latitudes and smaller G × E at higher latitudes. For example, at 35.7°N the magnitude of plasticity was ±16 days and ±10 days at 46.9°N (Fig. S2).

Table 2 Random effect variances and fixed effect parameters from linear mixed model analysis of *Artemisia tridentata* flower phenology

Random effects	Obs	Variance	SD	*P* value
Garden	3	70.95	8.42	$<2^{e-16}$
Population × garden	148	17.43	4.18	$<2^{e-16}$
Residual		39.15	6.26	
Fixed effects		**Estimate**	**SE**	***P* value**
Intercept		388.962	7.525	1.49^{e-14}
Latitude (photoperiod)		−1.949	0.120	$<2^{e-16}$
D100		−0.355	0.023	$<2^{e-16}$

D100 is the Julian date of accumulation of degree-days >5 °C reaching 100. Latitude is a surrogate for photoperiod.

The Julian dates of predicted flowering were mapped within the climatic niche of *A.t. wyomingensis* using the fixed effect intercept and slopes of latitude and D100 (Table 2). The *wyomingensis* niche model predicts a 66-day range in flowering from mid-August through mid-October (Julian date 227 to 293) for the contemporary climate. The mapped model predicts later flowering dates from areas of lower latitudes and earlier spring onset, whereas earlier flowering occurs in areas of higher latitudes and later spring onset (Fig. 3a). Mid-century (2060) and end-century (2090) maps show a considerable reduction in the climatic niche and a more constricted range in flowering, 58 days and 51 days, respectively (Fig. 3b, c).

Flowering date change across the distribution of *A. tridentata* ssp. *wyomingensis* was evaluated by subtracting decade 2060 and 2090 flowering date predictions from the contemporary prediction (Fig. 3a). The change in flowering date from contemporary to decades 2060 and 2090, without taking into account climatic

Table 1 Geographic and climatic attributes of the common gardens

Garden	Lat.	Long.	Elevation (m)	MTCM (°C)	MTWM (°C)	D100 (Julian date)
Majors Flat	39.339	−111.520	2105	−4.7	20.8	107
Ephraim	39.369	−111.578	1690	−9.7	21.2	85
Orchard	43.322	−115.998	974	−2.9	25.0	71

MTCM, mean temperature of the cold month; MTWM, mean temperature of the warmest month; D100 = Julian date of degree-days >5 °C reaching 100 are derived weather station data from 2011 to 2013.

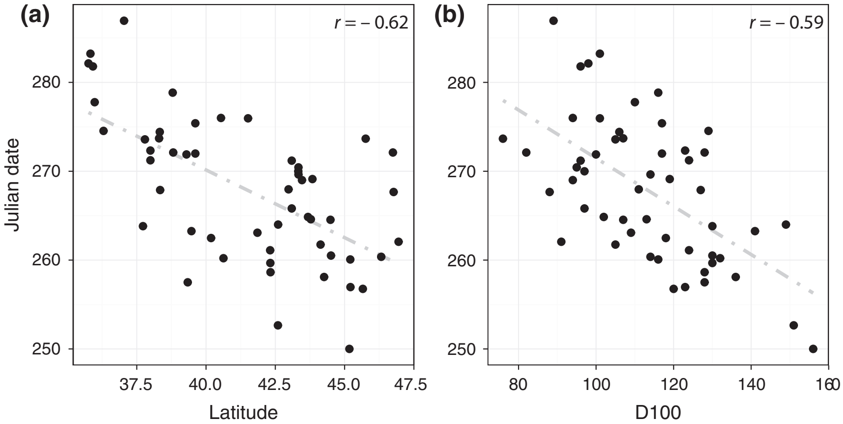

Fig. 1 Mean flowering Julian date of each *Artemisia tridentata* population plotted with: (a) latitude and (b) D100. These variables best explained the genetic variation used in the linear mixed-effects model (Table 2). Pearson's correlation coefficients (*r*) are provided in the upper right-hand corner of each panel. Note: Latitude is a surrogate for photoperiod, and D100 is the Julian date of degree-day >5 °C accumulating to 100.

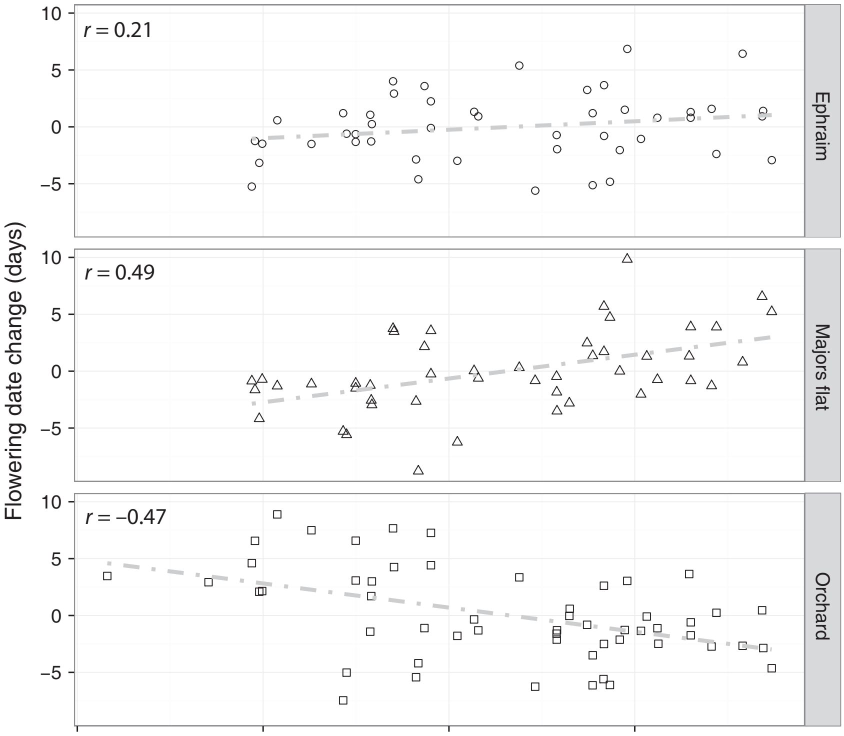

Fig. 2 Contrasting genotype-by-environment interaction (G × E) effects on flower phenology of *Artemisia tridentata* at warm and cold environments. The effect of G × E is plotted with latitude of the seed source location for each garden. Lower-latitude populations show greater plasticity to delay flowering in a warm environment (Orchard garden), and higher-latitude populations show greater plasticity to delay flowering in a cold environment (Majors Flat garden). Pearson's correlation coefficients (*r*) are reported in the upper left corner. Note that latitude is a surrogate for photoperiod.

niche loss, shows flowering date is delayed up to 10 days by 2060 (Fig. 4a) and 14 days by 2090 (Fig. 4b). However, areas with the largest flowering date change are largely masked by climatic niche loss in the southern portion of contemporary distribution. These maps illustrate that the predicted change across this distribution

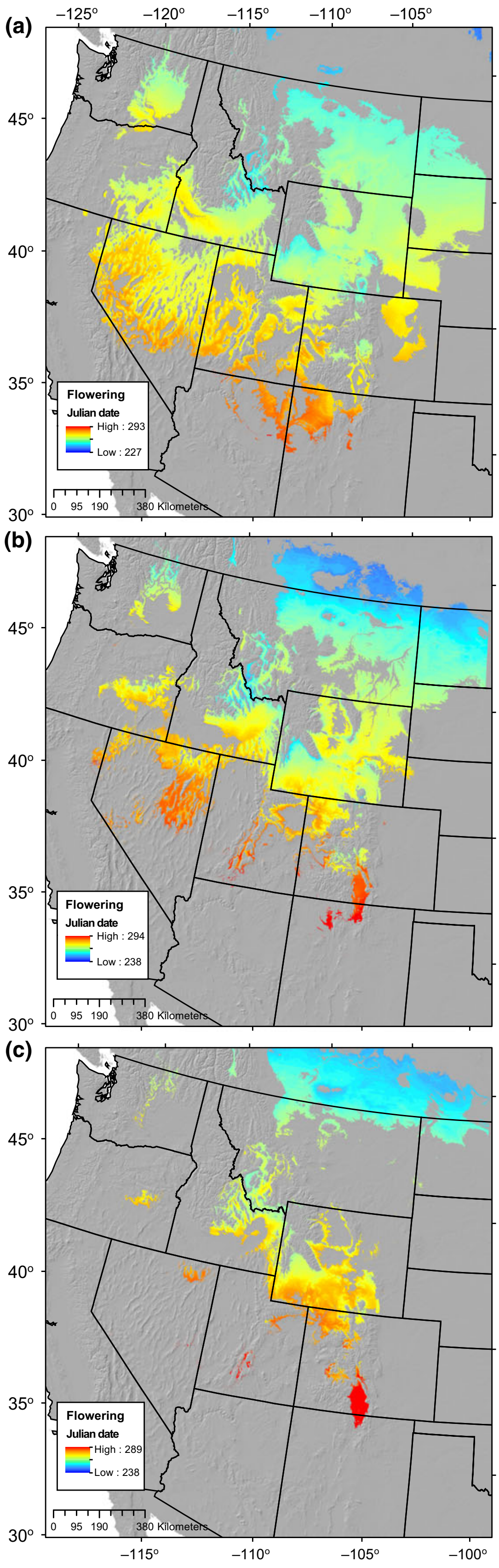

Fig. 3 Mapped model of flowering Julian date of *Artemisia tridentata* displayed within the climatic niche of subspecies *wyomingensis* for three time periods: (a) contemporary climate (1961–1990), and the decade surrounding (b) 2060 and (c) 2090. The color gradient depicts the clinal variation from earlier flowering (blue) to later flowering (red) for each respective time period. [Color figure can be viewed at wileyonlinelibrary.com].

varies from 2-day to 8-day delay by mid-century and 3-day to 11-day delay by end-century. Generally, the more continental and northerly regions east of the Rocky Mountains change less than the Great Basin (Fig. 4). The maps also illustrate that the flowering date change only exceeds plasticity thresholds (+13 days) by 2090 and in a small area (ca. 7700 km^2) of the Great Basin (Fig. 4b). Two populations from high and low latitudes (MTW1 and UTV2) were used as reference points to calculate climatypes to assess the combined effects genetics, plasticity and change in climatic niche. Confidence intervals adjusted for G × E were ±10.7 and ±14.8 days for high and low latitudes, respectively. The map illustrates the breadth of plasticity showing a large overlap between climatypes shown in yellow and that the coverage of two climatypes fills nearly all the climatic niche of *A.t. wyomingensis* (Fig. 5a). Climate futures show the decline in *A.t. wyomingensis*, especially of the southern climatypes (Fig. 5b, c).

Discussion

Populations of *A. tridentata* from cooler and more northerly sites flower earlier in the autumn compared to warmer, southerly sites. This cline in flower phenology was best explained by latitude and temperatures reflecting spring onset (Fig. 1). These predictor variables likely reflect photoperiod and vernalization controls. Photoperiod and vernalization have been well studied and implicated in model plants (Amasino, 2010; Song *et al.*, 2015). Moreover, similar to other autumn-flowering plants, the flowering date is negatively associated with latitude (Kawakami *et al.*, 2011). These environmental cues explaining the genetic variation accounted for a substantial amount (33%) of the total variation in flower phenology. Strong genetic responses in flower phenology have also been observed in short-lived plants (Franks, 2011; Galloway & Burgess, 2012). When mapped within the contemporary climatic niche of subspecies *wyomingensis*, our model suggests the cline in flowering date ranges 66 days (Fig. 3a), but this range is limited by 2090 (51 days) due to the reduction in the climatic niche (Fig. 3c).

Phenotypic plasticity has a substantial effect on the flower phenology of *A. tridentata*. Plasticity and G × E

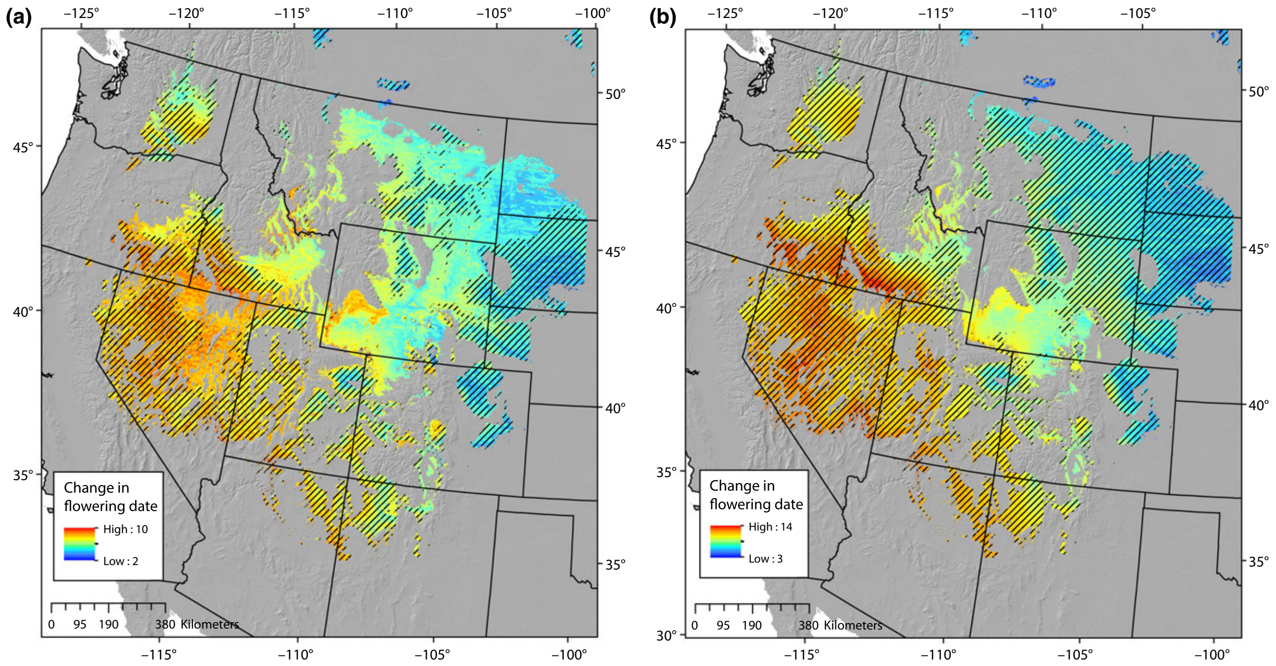

Fig. 4 Projected change in flowering date between the following: (a) contemporary and mid-century predictions (years 2046–2065) and (b) contemporary and end-century (years 2086–2095). The diagonal hatching shows predicted unsuitable climatic niche.
Note: Only contracting and stable climatic niches are shown, and areas of niche expansion are omitted. [Color figure can be viewed at wileyonlinelibrary.com].

explain 46% of the variation in flowering date, which is comparable to reports of bud burst (Vitasse *et al.*, 2013). An important component for assessing a species vulnerability to climate change involves estimating the magnitude of plasticity (Shaw & Etterson, 2012). Here, we use a similar approach of Rehfeldt *et al.* (2014a) to estimate climatypes by partitioning the clinal variation using confidence intervals surrounding the predicted mean flowering date of each population. Our analysis shows that on average, plasticity can change flowering date by ±13 days. In terms of climate, the Julian date of spring (D100) would have to change over a month (~36 days) for populations of *A. tridentata* to exceed their capacity to buffer temperature warming or cooling.

However, it is important to note that the genetic variation in plasticity (i.e., G × E) was significant and not uniform among populations. Under warmer conditions at the Orchard garden, lower-latitude populations were able to protract anthesis compared to higher-latitude populations. In contrast, under colder conditions at Majors Flat and Ephraim gardens, the lower-latitude populations tended to have more accelerated anthesis compared to higher-latitude populations (Fig. 2). The G × E pattern in *A. tridentata* may be a result of the varying sensitivity to photoperiod and vernalization that have been elucidated in *Arabidopsis* and wheat (Song *et al.*, 2015). In our study, the accelerated anthesis response of higher-latitude populations in a warmer climate (i.e., more photoperiod sensitive, Fig. S2) could be a conservative adaptive strategy to ensure flowering and seed development are completed before inclement weather in autumn. Autumn-freezing temperatures can be more variable at higher latitudes and locations with continental climates. On the other hand, protracted anthesis of lower-latitude populations (i.e., more temperature sensitive) in a warmer climate could be an adaptive strategy to ensure that seed matures and imbibes during winter when there are more sustained periods of available soil water.

The warmer conditions at the Orchard garden are likely to be more representative of the temperature warming and many *A. tridentata* populations will experience later this century. Therefore, the G × E influence on magnitude of plasticity at the Orchard garden would likely be indicative of projected temperature warming. In this case, the negative relationship between G × E and latitude at Orchard (slope = –0.42, Fig. 2) would result in more constricted plasticity at the highest latitudes. For example, the estimated phenotypic plasticity based on this linear model would be limited to ±10 days at the highest latitudes (46°N). However, plasticity would increase to ±16 days at the lowest latitude (35°N, Fig. 3). Similar findings of variation in plasticity have been reported in budburst phenology (Vitasse *et al.*, 2013), suggesting that plant

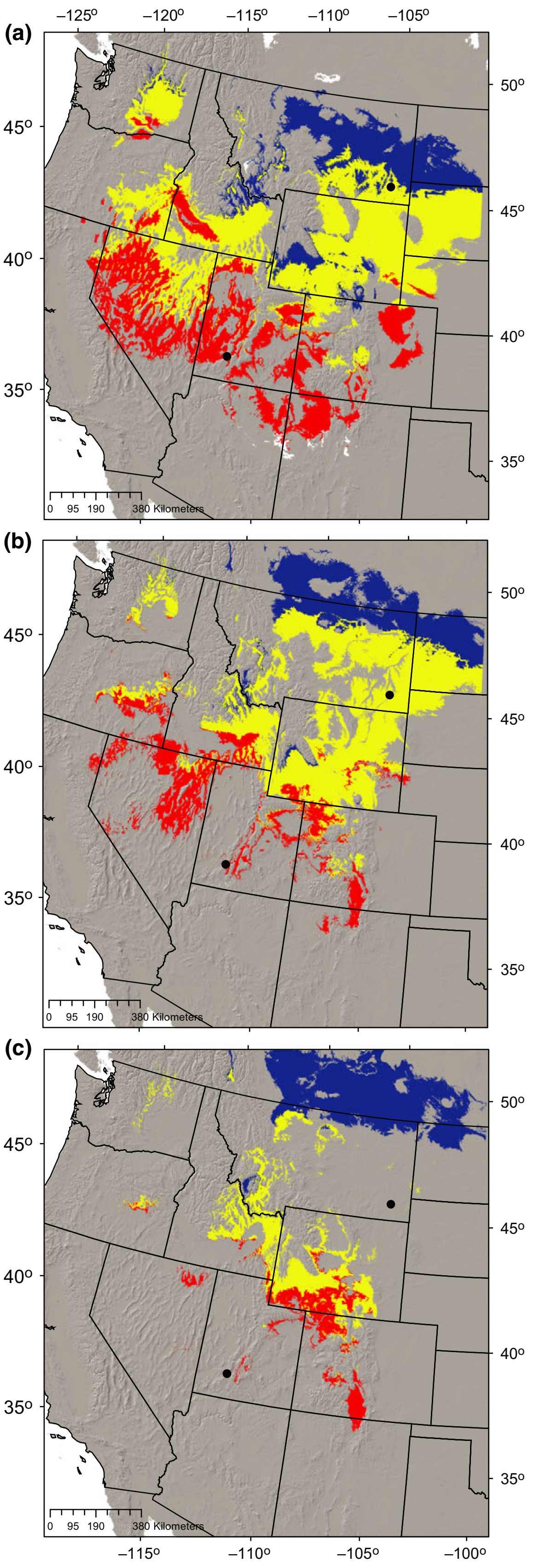

Fig. 5 Climatypes for two populations of *Artemisia tridentata* ssp. *wyomingensis* for (a) contemporary, (b) mid-century and (c) end-century climates. Red and blue colors indicate climatypes for southern and northern latitude populations, respectively. Yellow indicates overlap between climatypes, and white shows areas outside of both climatypes but within the climatic niche. Points indicate the location of the reference populations (MTW1 and UTV2, Table S1) used to build climatypes. [Color figure can be viewed at wileyonlinelibrary.com].

species with greater photoperiod sensitivity may have a more restricted trait response (Way & Montgomery, 2015). Moreover, Wang *et al.* (2014) found greater phenological sensitivity to temperature from areas with less spring temperature variance and less sensitivity in areas with high-temperature variance. The decline in temperature sensitivity was suggested to be a result of greater reliance on photoperiod controls. This variation in phenotypic plasticity will necessitate integration into the development of climatypes and seed transfer zones. In the case of *A. tridentata*, narrower climatypes are required at northern latitudes and wider climatypes at southern latitudes.

How much change in flowering date can be expected? To address this question, we map the landscape patterns of flowering date change expected for mid- and end-century. Flowering date is expected to be delayed 2–10 days by the mid-century (Fig. 4a) and 3–14 days by the end-century (Fig. 4b). There are regional differences in the change of flowering date. In the western regions of *A.t. wyomingensis* (i.e., the Great Basin), the flowering date change is expected to be higher compared to eastern regions (i.e., Rocky Mountains and northern Great Plains). In some areas, this predicted change threatens the limits of plasticity (+13 days). However, it is important to note that much of the climatic niche is lost in the Great Basin where higher flowering date change is predicted (Fig. 4).

Can plasticity accommodate rising temperatures? We constructed climatypes for two populations from high (MTW1) and low (UTV2) latitudes. The breadth of climatypes was large. These two populations can accommodate approximately 51 days of variation in flower phenology. Considering that the climatic niche of *A.t. wyomingensis* covers 66 days (Fig. 3a), the two climatypes can account for 77% of the variation in phenology. The climatypes also have a large overlap (Fig. 5). This suggests that plasticity can accommodate rising temperatures expected this century and even among northerly populations that are predicted to have a narrower breadth due to G × E response under warming temperatures (Fig. 2). Climatic niche modeling supports a large range contraction for *A.t. wyomingensis* and both climatypes (Fig. 5a, b), suggesting other life history traits are much more vulnerable to climate change.

Changes in flower phenology can have important effects on related traits and ecological interactions. For example, Galloway & Burgess (2009, 2012) have shown changing flowering date can affect other traits and the life histories of offspring. While such studies have not been conducted in *A. tridentata*, related traits like the timing of seed dispersal have to be synchronous with the window of suitable weather for germination and seedling establishment. In cold deserts where *A. tridentata* dominates, opportunities to imbibe and germinate can be episodic and occur between late winter and early spring when there is a convergence of suitable soil water and temperature (Meyer, 1994; Schlaepfer *et al.*, 2014). If flowering date and subsequent seed dispersal become misaligned with suitable weather events for germination and establishment, then plasticity or genetic responses for delayed flowering may result in poor fitness. Such a scenario could become increasingly plausible under climate warming. Studies using climatic niche models and mechanistic ecohydrology models suggest declining opportunities for sagebrush suitability and seedling establishment. These different models show that the trailing (southern) edge of sagebrush taxa is contracting due to increasing aridity (Still & Richardson, 2015) and decreasing soil water (Schlaepfer *et al.*, 2015; Palmquist *et al.*, 2016). It is possible that delayed flowering and subsequent seed development could have a negative feedback by limiting the opportunities sagebrush seed can imbibe and establish under favorable conditions.

Our analyses suggest that flower phenology in *A. tridentata* has the capacity via plasticity to adapt to climate change expected at mid- and end-century. While flowering phenology does not directly appear to be a limiting factor to the projected loss of suitable climatic niche later this century, the delay in flowering could have downstream consequences for seed and seedling traits. These associated traits could be limiting for *A. tridentata* establishment. Studies that develop an understanding of the linkage between traits will be important in assessing the vulnerabilities to climate change.

Acknowledgements

Funding was provided by the DOI Bureau of Land Management, Great Basin Native Plant Program and the USDA Forest Service, National Fire Plan. Thanks to the Utah Department of Natural Resources, Stephanie Carlson, Alexis Malcomb and Matt Fisk for data collection, and insightful comments from T. Tobiasson, A. Boyd and anonymous reviewers. Any use of trade, product or firm names is for descriptive purposes only and does not imply endorsement by the US Government.

References

Amasino R (2010) Seasonal and developmental timing of flowering. *The Plant Journal*, **61**, 1001–1013.

Anderson JT, Gezon ZJ (2014) Plasticity in functional traits in the context of climate change: a case study of the subalpine forb *Boechera stricta* (Brassicaceae). *Global Change Biology*, **21**, 1689–1703.

Anderson JT, Inouye DW, McKinney AM, Colautti RI, Mitchell-Olds T (2012) Phenotypic plasticity and adaptive evolution contribute to advancing flowering phenology in response to climate change. *Proceedings of the Royal Society B: Biological Sciences*, **279**, 3843–3852.

Bartoń K (2015) MuMIn: Multi-Model Inference. R package version 1.15.1. Available at: http://CRAN.R-project.org/package=MuMIn (accessed 7 March 2016).

Bates D, Maechler M, Bolker B, Walker S (2014) lme4: Linear mixed-effects models using Eigen and S4. R package version 1.1-7. Available at: http://CRAN.R-project.org/package=lme4 (accessed 7 March 2016).

Blackman BK, Michaels SD, Rieseberg LH (2011) Connecting the sun to flowering in sunflower adaptation. *Molecular Ecology*, **20**, 3503–3512.

Bolker BM, Brooks ME, Clark CJ, Geange SW, Poulsen JR, Stevens MHH, White J-SS (2009) Generalized linear mixed models: a practical guide for ecology and evolution. *Trends in Ecology & Evolution*, **24**, 127–135.

Crookston NL, Finley AO (2008) yaImpute: an R package for kNN imputation. *Journal of Statistical Software*, **23**, 1–16.

Crookston NL, Rehfeldt GE (2008) Climate estimates and plant-climate relationships. USDA Forest Service, Rocky Mountain Research Station, Moscow Idaho, USA. Available at: http://charcoal.cnre.vt.edu/climate/ (accessed 4 January 2016).

Elzinga JA, Atlan A, Biere A, Gigord L, Weis AE, Bernasconi G (2007) Time after time: flowering phenology and biotic interactions. *Trends in Ecology & Evolution*, **22**, 432–439.

Franks SJ (2011) Plasticity and evolution in drought avoidance and escape in the annual plant *Brassica rapa*. *New Phytologist*, **190**, 249–257.

Franks SJ (2015) The unique and multifaceted importance of the timing of flowering. *American Journal of Botany*, **102**, 1401–1402.

Franks SJ, Sim S, Weis AE (2007) Rapid evolution of flowering time by an annual plant in response to a climate fluctuation. *Proceedings of the National Academy of Sciences of the United States of America*, **104**, 1278–1282.

Franks SJ, Weber JJ, Aitken SN (2013) Evolutionary and plastic responses to climate change in terrestrial plant populations. *Evolutionary Applications*, **7**, 123–139.

Galloway LF, Burgess KS (2009) Manipulation of flowering time: phenological integration and maternal effects. *Ecology*, **90**, 2139–2148.

Galloway LF, Burgess KS (2012) Artificial selection on flowering time: influence on reproductive phenology across natural light environments. *Journal of Ecology*, **100**, 852–861.

Gordo O, Sanz JJ (2010) Impact of climate change on plant phenology in Mediterranean ecosystems. *Global Change Biology*, **16**, 1082–1106.

Haggerty BP, Galloway LF (2010) Response of individual components of reproductive phenology to growing season length in a monocarpic herb. *Journal of Ecology*, **99**, 242–253.

Hutchinson MF (2004) Hutchinson: ANUSPLIN Version 4.3. User's guide. Centre for Resource and Environmental Studies, Australian National University, Canberra, Australia.

Jaeger DM, Runyon JB, Richardson BA (2016) Signals of speciation: volatile organic compounds resolve closely related sagebrush taxa, suggesting their importance in evolution. *New Phytologist*, **211**, 1393–1401.

Johnson PCD (2014) Extension of Nakagawa & Schielzeth's R2GLMM to random slopes models (ed O'Hara RB). *Methods in Ecology and Evolution*, **5**, 944–946.

Joyce DG, Rehfeldt GE (2013) Climatic niche, ecological genetics, and impact of climate change on eastern white pine (*Pinus strobus* L.): guidelines for land managers. *Forest Ecology and Management*, **295**, 173–192.

Kawakami T, Morgan TJ, Nippert JB, Ocheltree TW, Keith R, Dhakal P, Ungerer MC (2011) Natural selection drives clinal life history patterns in the perennial sunflower species, *Helianthus maximiliani*. *Molecular Ecology*, **20**, 2318–2328.

Körner C, Basler D (2010) Phenology under global warming. *Science*, **327**, 1461–1462.

Kuznetsova A, Brockhoff PB, Christensen RHB (2016) lmerTest: tests for random and fixed effects for linear mixed effect models. R package version 2.0-30. Available at: http://CRAN.R-project.org/package=lmerTest (accessed 7 March 2016).

Langlet O (1971) Two hundred years genecology. *Taxon*, **20**, 653.

Laube J, Sparks TH, Estrella N, Höfler J, Ankerst DP, Menzel A (2014) Chilling outweighs photoperiod in preventing precocious spring development. *Global Change Biology*, **20**, 170–182.

McArthur ED, Sanderson SC (1999) Cytogeography and chromosome evolution of subgenus *Tridentatae* of *Artemisia* (Asteraceae). *American Journal of Botany*, **86**, 1754–1775.

Menzel A, Sparks TH, Estrella N *et al.* (2006) European phenological response to climate change matches the warming pattern. *Global Change Biology*, **12**, 1969–1976.

Meyer SE (1994) Germination and establishment ecology of big sagebrush: implications for community restoration. In: *Proceedings of Ecology and Management of Annual Rangelands* (eds Monsen SB, Kitchen SG), pp. 244–252. INT-GTR-313, USDA Forest Service, Intermountain Research Station, Ogden, UT.

Morgenstern EK (1996) *Geographic Variation in Forest Trees: Genetic Basis and Application of Knowledge in Silviculture*. UBC Press, Vancouver.

Palmquist KA, Schlaepfer DR, Bradford JB, Lauenroth WK (2016) Mid-latitude shrub steppe plant communities: climate change consequences for soil water resources. *Ecology*, **97**, 2342–2354.

Parmesan C, Yohe G (2003) A globally coherent fingerprint of climate change impacts across natural systems. *Nature*, **421**, 37–42.

Pigliucci M (2005) Evolution of phenotypic plasticity: where are we going now? *Trends in Ecology & Evolution*, **20**, 481–486.

R Core Team (2015) *R: A Language and Environment for Statistical Computing*. R Foundation for Statistical Computing, Vienna, Austria. Avaliable at: http://www.R-project.org/ (accessed 21 June 2016).

Rehfeldt GE (2006) A spline model of climate for the western United States. General Technical Report RMRS-GTR-165. USDA Forest Service, Rocky Mountain Research Station, Fort Collins, Colorado, USA.

Rehfeldt GE, Jaquish BC, Sáenz-Romero C, Joyce DG, Leites LP, St Clair JB, López-Upton J (2014a) Comparative genetic responses to climate in the varieties of *Pinus ponderosa* and *Pseudotsuga menziesii*: realized climate niches. *Forest Ecology and Management*, **324**, 126–137.

Rehfeldt GE, Leites LP, St Clair JB, Jaquish BC, Sáenz-Romero C, López-Upton J, Joyce DG (2014b) Comparative genetic responses to climate in the varieties of *Pinus ponderosa* and *Pseudotsuga menziesii*: clines in growth potential. *Forest Ecology and Management*, **324**, 138–146.

Richardson BA, Page JT, Bajgain P, Sanderson SC, Udall JA (2012) Deep sequencing of amplicons reveals widespread intraspecific hybridization and multiple origins of polyploidy in big sagebrush (*Artemisia tridentata*; Asteraceae). *American Journal of Botany*, **99**, 1962–1975.

Richardson BA, Ortiz HG, Carlson SL, Jaeger DM, Shaw NL (2015) Genetic and environmental effects on seed weight in subspecies of big sagebrush: applications for restoration. *Ecosphere*, **6**, art201–art213.

Schielzeth H, Nakagawa S (2012) Nested by design: model fitting and interpretation in a mixed model era. *Methods in Ecology and Evolution*, **4**, 14–24.

Schlaepfer DR, Lauenroth WK, Bradford JB (2014) Natural regeneration processes in big sagebrush (*Artemisia tridentata*). *Rangeland Ecology & Management*, **67**, 344–357.

Schlaepfer DR, Taylor KA, Pennington VE *et al.* (2015) Simulated big sagebrush regeneration supports predicted changes at the trailing and leading edges of distribution shifts. *Ecosphere*, **6**, art3.

Shaw RG, Etterson JR (2012) Rapid climate change and the rate of adaptation: insight from experimental quantitative genetics. *New Phytologist*, **195**, 752–765.

Song YH, Shim JS, Kinmonth-Schultz HA, Imaizumi T (2015) Photoperiodic flowering: time measurement mechanisms in leaves. *Annual Review of Plant Biology*, **66**, 441–464.

Stevens R, McArthur E (1974) A simple field technique for identification of some sagebrush taxa. *Journal of Range Management*, **27**, 325–326.

Still SM, Richardson BA (2015) Projections of contemporary and future climate niche for Wyoming big sagebrush (*Artemisia tridentata* subsp. *wyomingensis*): a guide for restoration. *Natural Areas Journal*, **35**, 30–43.

Vitasse Y, Hoch G, Randin CF, Lenz A, Kollas C, Scheepens JF, Körner C (2013) Elevational adaptation and plasticity in seedling phenology of temperate deciduous tree species. *Oecologia*, **171**, 663–678.

Viveros-Viveros H, Sáenz-Romero C, Vargas-Hernández JJ, López-Upton J, Ramírez-Valverde G, Santacruz-Varela A (2009) Altitudinal genetic variation in *Pinus hartwegii* Lindl. I: height growth, shoot phenology, and frost damage in seedlings. *Forest Ecology and Management*, **257**, 836–842.

van Vuuren DP, Edmonds J, Kainuma M *et al.* (2011) The representative concentration pathways: an overview. *Climatic Change*, **109**, 5–31.

Wang T, Ottlé C, Peng S *et al.* (2014) The influence of local spring temperature variance on temperature sensitivity of spring phenology. *Global Change Biology*, **20**, 1473–1480.

Way DA, Montgomery RA (2015) Photoperiod constraints on tree phenology, performance and migration in a warming world. *Plant, Cell and Environment*, **38**, 1725–1736.

Wilczek AM, Roe JL, Knapp MC *et al.* (2009) Effects of genetic perturbation on seasonal life history plasticity. *Science*, **323**, 930–934.

Wilczek AM, Burghardt LT, Cobb AR, Cooper MD, Welch SM, Schmitt J (2010) Genetic and physiological bases for phenological responses to current and predicted climates. *Philosophical Transactions of the Royal Society of London B: Biological Sciences*, **365**, 3129–3147.

Supporting Information

Additional Supporting Information may be found in the online version of this article:

Figure S1. Mean flowering date (Julian date) is plotted for each population.
Figure S2. The predicted mean flower date is plotted with latitude for each population of *Artemisia tridentata*.
Table S1. Geographic and subspecies information of the seed collection sites (populations) and sample size (*N*) found in each common garden (Ephraim, Majors Flat and Orchard).
Table S2. Calculated confidence intervals for individual populations.